Screening and electronic correlations in quantum wires in strong magnetic fields: Filling factor dependence

Zhongxi Zhang† and P. Vasilopoulos*
Department of Physics, Concordia University, 1455 de Maisonneuve Ouest, Montréal, Québec, H3G 1M8, Canada
(Received 3 July 2002; published 27 November 2002)

The screening of the Coulomb interaction in quantum wires, subjected to strong perpendicular magnetic fields, is assessed for integer filling factors $\nu \leqslant 3$ and low temperatures. Correlations due to bulk screening are rather weak whereas those due to screening at the edges are very strong and smoothen considerably the energy dispersion. The group velocity at the Fermi edge $v_g(k_{F\nu})$ can be one order of magnitude larger than the Hartree velocity $v_g^{\mathrm{H}}(k_{F\nu})$. The exchange-correlation contribution $v_g^{\mathrm{ec}}(k_F)$ to $v_g(k_F)$ is proved to be nonsingular and for sufficiently strong magnetic fields $v_g^{\mathrm{ec}}(k_F)$ is proportional to $v_g^{\mathrm{H}}(k_{F\nu})$ with a proportionality constant that depends on ν. The dispersion relation, obtained in the screened Hartree-Fock approximation, is in line with the observed strong suppression of the spin splitting for $\nu=1$ and helps explain the observed destruction or absence of some quantum Hall states. For $\nu=2$ the effective g_{op}^* factor is constant whereas for $\nu=1(3)$ varies strongly across the channel. In addition, the calculated activation energies agree well with those determined experimentally.

DOI: 10.1103/PhysRevB.66.205322 PACS number(s): 72.20.−i, 72.30.+q, 73.20.Mf

I. INTRODUCTION

Though most of the recent theoretical work has focused on the edge-state properties in the quantum Hall regime,[1–4] the influence of electron–electron interactions on the subband structure of quantum wires (QW) in the presence of strong magnetic fields has been studied extensively.[4–8] To date we are aware of treatments of a Coulomb interaction within the Hartree,[1,6] the Hartree-Fock,[5] and the screened Hartree-Fock approximations (SHFA).[12,8,10] One important conclusion of Ref. 8 is that electronic correlations in submicron-width channels strongly suppress the exchange splitting and smoothen the energy dispersion near the Fermi edge, where the derivative of the exchange contribution diverges logarithmically. This is similar to the case of a three-dimensional (3D) free electron gas. As is well known, the unphysical singularity of the Hartree-Fock energy can be traced back to the divergence of the Fourier transform of the bare Coulomb potential $4\pi e^2/q^2$ at $\mathbf{q}=0$, and it can be removed by taking into account the screening effects of other electrons in the system. However, in a quantum wire subjected to a strong perpendicular magnetic field, it is not *a priori* clear how the singularity at the Fermi level caused by exchange is canceled by the screening and what the properties of the screening field are. In a previous paper[9] we showed how this is brought about by means of approximate analytical and near-exact numerical calculations. The results for the energy dispersion curves were in agreement with experimental results.[7]

The results of Ref. 8 are in reasonable agreement with some experimental results[7] though they were obtained by an incomplete iteration procedure. Moreover, as discussed in Ref. 8 the validity of some of the nonstandard approximations made is not obvious for $r_0 \sim 1$, where $r_0 = e^2/(\epsilon l_0 \hbar \omega_c)$. The improvement of the iteration procedure of Ref. 9 led to results for the correlation energies that were not much different than those of Ref. 8. Moreover, the procedure of Ref. 9 did show how the singularity of the exchange energy could be avoided when correlations are taken into account. Also, the results of Ref. 9 were obtained without the assumption $r_0 \ll 1$ common to standard perturbative calculations.

All the works mentioned above, however, are valid only for $\nu=1$, where ν is the filling factor. As is well known though from studies of the g^* factor of the two-dimensional electron gas (2DEG),[12,13] the screening properties change substantially when a partially occupied Landau level (LL) becomes fully occupied. Thus, it is of interest to assess the influence of the filling factor on the screening and many-body effects in quantum wires as thoroughly as possible. We provide such an assessment also because we are not aware of any pertinent treatment for quantum wires and because that of Refs. 8,10 does not appear to be easily amenable to generalization. In contrast, the treatment of Ref. 9 can be extended to cases with a $\nu>1$, ν integer, albeit with some additional work.

The derivative, with respect to the wavenumber, of the single-particle energy near the channel edge is the key parameter in self-consistent studies of the edge screening effects,[8,10] of the edge magnetoplasmons (EMP)[11] as it is related to experimental observations, etc.[7] Though there was a certain progress in this respect,[3,8–11] it is worth studying the subject further and obtaining results as explicit as possible.

In this work we consider submicron channels of width W with abrupt boundaries (obtained by etching techniques) that prevent flattening of the edge states of the lower $(n=0,1)$ occupied Landau levels (LLs).[3,4,6] For the assumed integral quantum Hall Effect (IQHE) states in such channels, since the edge electrons of each occupied subband are very close to the channel boundaries, the effect of the compressive charge phase[3] suggested for the smooth boundaries can be neglected.[4] As a result, for samples with a parabolic confining potential, there is a simple relation between the integer filling factor ν of the QHE states and the corresponding magnetic fields B_ν, i.e., $B_\nu \nu = \mathrm{const}$, as observed in some experimental studies; cf. Ref. 7 for $\nu \leqslant 4$ and sample 1.

The paper is organized as follows. In Secs. II and III we briefly present the formalism and obtain an approximate analytical solution of the integral equation for the screened potential, for $\nu=1,2,3$; we confirm it by presenting the corresponding numerical solution. In Sec. IV we use the analytical solution to calculate the correlation energies based on the SHFA and show how the divergence in the group velocity at the Fermi edge, due to exchange, is canceled by that due to correlations. In addition, we obtain new expressions for the Fermi edge slope of the exchange-correlation energies. Further, we obtain the single-particle energy by generalizing the mean-field approach of Ref. 8 for $\nu=1$ to $\nu\leqslant 3$. Concluding remarks follow in Sec. V.

II. BASIC FORMULAS

We consider a QW in the $x-y$ plane, with the unconstrained electron motion along the axis (x) of the QW and a magnetic field B in the z direction. For a narrow QW of width $W\sim 0.3$ μm, we assume that the confining potential V_y, in the Hartree approximation,[7,8] is parabolic, $V_y=m^*\Omega^2 y^2/2$, for $|y|\leqslant W/2$ and has an infinite height for $|y|>W/2$; m^* is the effective mass. With the vector potential $\vec{A}=(-By,0,0)$ the one-electron Hamiltonian,

$$h^0=\frac{p_y^2}{2m^*}+\frac{m^*\tilde{\omega}^2}{2}[y-y_0(p_x)]^2+\frac{p_x^2}{2\tilde{m}}+\frac{g_0\mu_B S_z B}{2}, \quad (1)$$

has the following eigenvalues and eigenfunctions:

$$\varepsilon_{\alpha\sigma}\equiv\varepsilon_{n,k_x,\sigma}=\hbar\tilde{\omega}(n+1/2)+\hbar^2k_x^2/2\tilde{m}+g_0\mu_B\sigma B/2, \quad (2)$$

$$\langle x,y|\alpha\rangle=e^{ik_x x}\Phi_n(y-y_0)|\sigma\rangle/\sqrt{L}, \quad (3)$$

with $\omega_c=|e|B/m^*$, $\tilde{\omega}=(\omega_c^2+\Omega^2)^{1/2}$, $\tilde{m}=m^*\tilde{\omega}^2/\Omega^2$, $y_0(p_x)=p_x\omega_c/(m^*\tilde{\omega}^2)$, and L the length of the channel. In Eq. (3) $\Phi_n(y-y_0(k_x))$ is the displaced harmonic oscillator function centered at $y_0\propto k_x$ and $|\sigma\rangle$ is the spin state vector satisfying $\langle\sigma_1|\sigma_2\rangle=\delta_{\sigma_1\sigma_2}$. For the calculation that follows we need the matrix elements decsibing transitions between the states $|n,k_x\rangle$ and $|n',k_x'\rangle$; they are given by[5,8]

$$\langle n'k_x'|e^{i\mathbf{q}\cdot\mathbf{r}}|nk_x\rangle=\delta_{q_x+k_-,0}(n'!/n!)^{1/2}\eta^{n-n'}e^{-u/2}\times L_{n'}^{n-n'}(u)e^{iaq_yk_+l^2/2}, \quad (4)$$

where $k_\pm=k_x\pm k_x'$, $a=\omega_c/\tilde{\omega}$, $\eta=l(-ak_-+iq_y)/\sqrt{2}$, $u=[a^2q_x^2+q_y^2]l^2/2$, and $l=(\hbar/m^*\tilde{\omega})^{1/2}$ is the magnetic length, and $L_{n'}^{n-n'}(u)$ the Laguerre polynomial. Due to momentum conservation k_x and k_x' should satisfy the relation $q_x+k_-=0$. In the y direction the factor $\exp(-u/2)$ means that transitions occur mainly in the long-wavelength region. This can be used to simplify the discussion of the screened field $V^s(q_x,q_y,q_y')$. The phase shift factor in the matrix element (4) results from the overlap between the two displaced Fock states.[14] It leads to the oscillations of the screened field in momentum space. With the help of the SHFA,[12,8] the exchange and correlation contribution $\varepsilon_{n,k_x,\sigma}^{ec}$ to the single-particle energy of the same spin state is given by

$$\varepsilon_{n,k_x,\sigma}^{ec}\approx-\frac{1}{8\pi^3}\sum_{n'}\int dk_x'\,dq_y\,dq_y'V^s(k_x-k_x',q_y,q_y')\times(n,k_x|e^{iq_yy}|n',k_x')(n',k_x'|e^{iq_y'y}|n,k_x), \quad (5)$$

where n' is the index of the occupied LLs. The sum over n' means that, for a given screened potential, the energy correction $\varepsilon_{n,k_x,\sigma}^{ec}$ results from the exchange between electrons of the given n LL and those of the filled $n'=0,1,2\ldots$, LLs. In Ref. 9 we treated only the $\nu=1$ case and took $n=n'=0$. Based on the classical 2D-Poisson equation and the random-phase approximation (RPA), the potential $V^s(k_-,q_y,q_y')$ in Eq. (5) obeys the integral equation

$$V^s(q_x,q_y,q_y')=\frac{v_0\,\delta(q_y+q_y')}{q}+\frac{v_0}{8\pi^3q}\int dq_{y1}\,V^s(q_x,q_{y1},q_y')\times\sum_{n_\alpha,n_\beta}\sum_{\sigma=\pm1}\int dk_{x\alpha}F_{\alpha,\beta}^{\sigma}(n_\alpha,k_{x\alpha}|e^{iq_{y1}y}|\times n_\beta,k_{x\alpha}-q_x)(n_\beta,k_{x\alpha}-q_x|e^{-iq_yy}|n_\alpha,k_{x\alpha}), \quad (6)$$

with $v_0=4\pi^2e^2/\epsilon$, $q^2=q_x^2+q_y^2$, $F_{\alpha,\beta}^{\sigma}=(f_\alpha-f_\beta)/(\varepsilon_\alpha-\varepsilon_\beta)$, and f_α the Fermi-Dirac function. In the limit of $W\to\infty$ Eq. (6) can be reduced to the standard Lindhard equation.[9] The overall field $V^s(q_x,q_y,q_y')$ can be decomposed in the manner

$$V^s(q_x,q_y,q_y')=v_0\delta(q_y+q_y')/q+V_c^s(q_x,q_y,q_y'). \quad (7)$$

The first term is the bare Coulomb potential and corresponds to the exchange energy. The second term, V_c^s, is caused by the induced charges due to transitions between the states α and β. This V_c^s corresponds to the correlation energy and satisfies a modified integral equation obtained readily from Eq. (6). In the following we will neglect the small Zeeman energy ($g_0\mu_BB/2|_{B=10T}\approx 0.01\hbar\omega_c$) and make the approximation $F_{\alpha,\beta}^{\pm1}\approx F_{\alpha,\beta}\equiv(f_\alpha^0-f_\beta^0)/(\varepsilon_\alpha-\varepsilon_\beta)$ with $f_\alpha^0=1/[1+\exp((\varepsilon_\alpha-E_F)/kT)]$.

III. SCREENED FIELD IN A QW FOR INTEGER FILLING FACTORS

For sufficiently strong magnetic fields B, such that $\tilde{\omega}l\gg v_g^H(k_{F\nu})$, a simplied integral equation can be obtained by considering only the intra-level and adjancent-level transitions in Eq. (6). For $T=0$ K and $a\approx 1$ we obtain

$$V_{c\nu}^s(q_x,q_y,q_y')=\frac{v_0v_1}{4\pi^3}\Phi(\tilde{q}_x,\tilde{q}_y)\Big[v_0\Phi(\tilde{q}_x,\tilde{q}_y')\times[P_{s\nu}(\tilde{q},\tilde{q}')\cos\tilde{k}_{F\nu}(\tilde{q}_y+\tilde{q}_y')-P_{a\nu}^-(\tilde{q},\tilde{q}')\mathrm{sinc}(\tilde{q}_y+\tilde{q}_y')]$$

$$+\int d\tilde{q}_{y_1} V^s_{c\nu}(q_x,q_{y_1},q'_y)\Phi(\tilde{q}_x,\tilde{q}_{y_1})$$
$$\times(\tilde{q}_1/l^2)[P_{s\nu}(\tilde{q},\tilde{q}_1)\cos\tilde{k}_{F\nu}(\tilde{q}_y-\tilde{q}_{y_1})$$
$$-P^{+}_{a\nu}(\tilde{q},\tilde{q}_1)\mathrm{sinc}(\tilde{q}_y-\tilde{q}_{y_1})]\Big]; \quad (8)$$

here $\tilde{Y}=Yl$, $v_1=-\tilde{m}/\hbar^2 k_{F\nu}\approx -1/[v_g^{HA}(k_{F\nu})\hbar]$, $\Phi(\tilde{q}_x,\tilde{q}_y)=(l/\tilde{q})\exp(-\tilde{q}^2/4)$, $\mathrm{sinc}(x)=\sin(x)/x$, and $P_{s\nu}(\tilde{q},\tilde{q}')$ is a polynomial associated with intra-level transitions; its form depends on ν. The other polynomial $P^{\pm}_{a\nu}=p_{a\nu}Q_{\pm}$, with $Q_{\pm}=(\tilde{q}_x^2\pm\tilde{q}_y\tilde{q}'_y)/\tilde{\omega}\hbar l v_1$, is associated with adjacent-level transitions. When the $n=0$ LL is occupied, the nonzero coefficients $F^{\sigma}_{\alpha,\beta}$ in Eq. (6) are $F^{\sigma}_{0,0},F^{\sigma}_{1,0}$, and $F^{\sigma}_{0,1}$ with $\sigma=1(\pm 1)$ for $\nu=1(2)$. Accordingly, we have $P_{s\nu}=p_{a\nu}=\nu$ in Eq. (8). For $\nu=3$, the coupling coefficients needed to be considered are $F^{\pm}_{1,0},F^{\pm}_{0,1},F^{1}_{2,1},F^{1}_{1,2},F^{\pm}_{0,0},F^{1}_{1,1}$. The first four coupling coeficients relate to adjacent-level transitions. They give $p_{a3}=2+2Q_4Q'_4$, with $Q_iQ'_i=(1-\tilde{q}^2/i)(1-\tilde{q}'^2/i)$, $i=2,4$. The last two coupling coeficients lead to $p_{s3}=2+Q_2Q'_2$; the term $\propto 2$ comes from the $n=0$ spin-up and spin-down LLs, and the second term from the $n=1$ spin-up LL. Notice that, for the same spin state, the intra-level transitions within the $n=1$ LL are slightly weaker than those within the $n=0$ LL. We expand this point further in Sec. IV and show that it is this small difference between these two kind of transitions that leads to a considerable difference between the Fermi-edge group velocities $v_g^{ec}(k_{F3})$ and $v_g^{ec}(k_{F1})$.

In deriving Eq. (8) we used the relation[9]

$$\int_{-\infty}^{\infty} dk_{x\alpha} F_{0,0} e^{-i(\tilde{q}_y+\tilde{q}'_y)(\tilde{k}_{x\alpha}-\tilde{q}_x/2)}\approx v_1 e^{i(\tilde{q}_y+\tilde{q}'_y)\tilde{k}_F}. \quad (9)$$

A slightly different result would be obtained if we used the approximation $F_{0,0}\approx -2\tilde{m}\delta(k_{x\alpha}^2-k_{F1}^2)/\hbar^2$ on the left-hand side of Eq. (9). The physical meaning of this approximation is that, at $T=0$ K, the intra-level transitions take place only *at* the edges of the channel whereas the fact is that all electrons *near* the edges contribute to the screening of the potential. Mathematically, this approximation would result in a small phase-shift factor $e^{i\tilde{q}_x(\tilde{q}_y+\tilde{q}'_y)/2}$ on the right-hand side of Eq. (9).[15] Using Eq. (9) will lead to results that are more accurate and closer to the experimental ones.

The right-hand side of Eq. (8), proportional to the total induced charge density, consists of two terms. The first term results from the unperturbed charge distribution. It consists of even and odd modes, pertinent to intra-level screening, and the sinc mode pertinent to inter-level screening. The second term is a further correction caused by the density change in the unperturbed electron distribution. If it can be written in a form similar to the first one, then Eq. (8) can be solved in an easier way. To confirm this we attempt an approximate analytic solution to Eq. (8) in the form

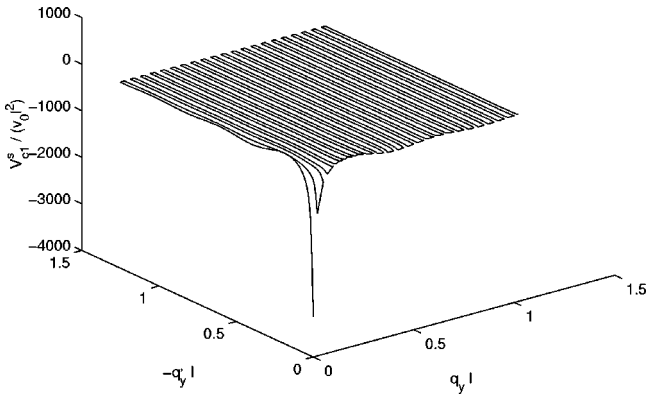

FIG. 1. The numerical solution (solid curve) and the analytic one (dashed curve) given by Eq. (10), pertinent to sample 1 of Ref. 7, with $\nu=1,\tilde{k}_{F1}=15,r_0=0.85$, $\Omega=\omega/25$, and $\tilde{q}_x=1/150$. The two solutions are nearly identical. In the long-wavelength region the solution tends to diverge.

$$V^s_{c\nu}(q_x,q_y,q'_y)=v_0\Phi(\tilde{q}_x,\tilde{q}_y)\Phi(\tilde{q}_x,\tilde{q}'_y)[\tilde{k}_{c\nu}cc'+\tilde{k}_{s\nu}ss'$$
$$+\tilde{k}_{sc\nu}Q_-(\tilde{q}'_y)\mathrm{sinc}(\tilde{q}_y+\tilde{q}'_y)], \quad (10)$$

where cc' stands for $\cos\tilde{k}_{F\nu}\tilde{q}_y\cos\tilde{k}_{F\nu}\tilde{q}'_y$ and ss' for $\sin\tilde{k}_{F\nu}\tilde{q}_y\sin\tilde{k}_{F\nu}\tilde{q}'_y$. The coefficients $\tilde{k}_{c\nu},\tilde{k}_{s\nu}$, and $\tilde{k}_{sc\nu}$ can be obtained by using the mode-match technique of Ref. 9. The results are given in Appendix A, for $\nu=1,2$, and B for $\nu=3$.

The numerical solution of Eq. (8) is obtained by using the weighted iterative method of Ref. 9. In Fig. 1 we plot the numerical solution of Eq. (8) as well as its analytic one, Eq. (10), for sample 1 of Ref. 7, i.e., $\nu=1,\tilde{q}_x=1/10\tilde{k}_{F1}=1/150,r_0=0.85$, and $\Omega=\omega/25$. As shown, the two solutions are nearly indistinquishable. Notice that in the long-wavelength region, $\tilde{q}\to 0$, the screened fields tend to diverge and this would invalidate the use of the normal iterative method. Figure 2 shows the two solutions with $\nu=2,\tilde{q}_x=1/\tilde{k}_{F2}=1/10.6,r_0=0.85$, and $\Omega=\omega/12.5$. From this figure we can see that even in the region of $\tilde{q}_x\sim 1/\tilde{k}_{F\nu}$, where the

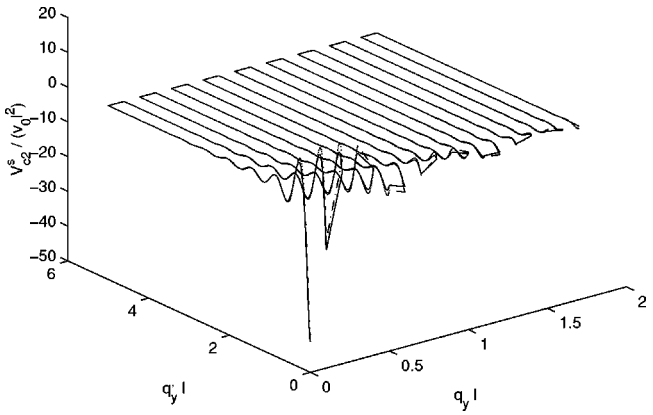

FIG. 2. As in Fig. 1 with $\nu=2,\tilde{k}_{F2}=10.6,\Omega=\omega/12.5$, and $\tilde{q}_x=1/\tilde{k}_{F2}=1/10.6$. There are visible but small differences between the two solutions.

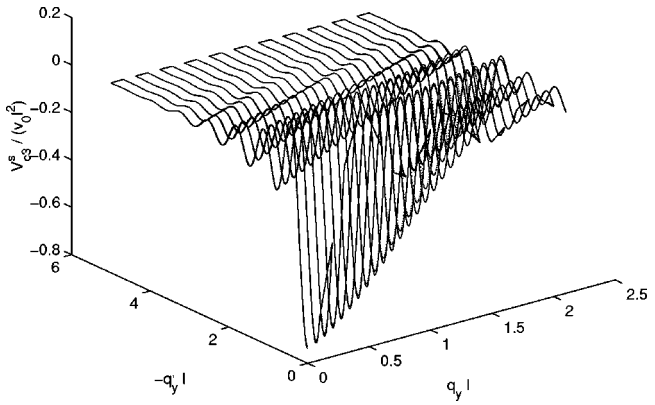

FIG. 3. The same as in Fig. 1 with $\nu=3, \tilde{k}_{F3}=8.66, \Omega=3\omega/25$, and $\tilde{q}_x=2$. The two solutions are nearly identical.

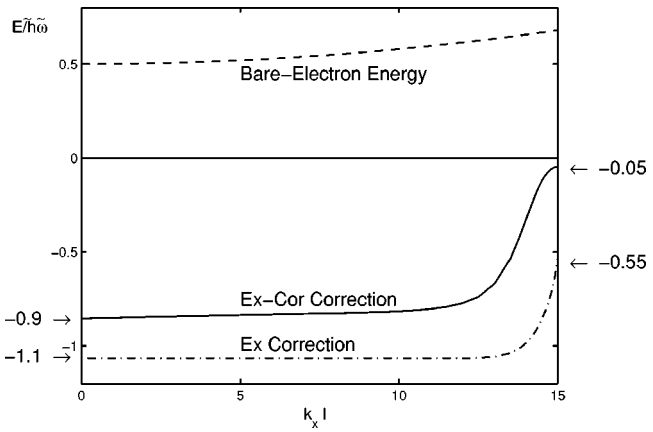

FIG. 4. Exchange energy (dash−dotted curve), given by Eq. (12), and the exchange-correlation energy (solid curve) for sample 1 of Ref. 7 with $\nu=1$. The difference between the two curves is the correlation correction given by Eq. (11). It is very strong near the edge of the channel and rather weak near its center. The dashed curve, given by Eq. (2), shows the electron energy without many-body effects.

accuracy of the analytic approximation is worst, we still have good agreement between the two solutions. Figure 3 shows that for $\tilde{q}_x=2$ the two solutions are, again, nearly identical. The general agreement between the two solutions, as indicated above and further specified in the appendices, validates Eq. (10) and the approximations made in obtaining the coefficients $\tilde{k}_{c\nu}, \tilde{k}_{s\nu}$, and $\tilde{k}_{sc\nu}$.

IV. EXCHANGE-CORRELATION ENERGY, ITS FERMI-EDGE SLOPE

A. $\nu=1,2$

Based on Eqs. (5), (7), and (10) we decompose the exchange-correlation correction $\varepsilon^{ec}_{0,k_x,1}$ into

$$\varepsilon^{co}_{0,k_x,1} \approx -2\overline{v}_0 I_-(\nu) \int\int d\tilde{q}_y\, d\tilde{q}'_y \times e^{i(\tilde{q}_y+\tilde{q}'_y)\tilde{k}_+/2} K_\nu \tilde{\Lambda}_- \tilde{\Lambda}'_- / \tilde{q}^2_- \tilde{q}'^2_- \tag{11}$$

and

$$\varepsilon^{ex}_{0,k_x,1} = -\overline{v}_0 I_+(\nu) \int d\tilde{q}_y\, \tilde{\Lambda}_- / \tilde{q}^2_-; \tag{12}$$

here $\overline{v}_0 = v_0/l4\pi^3$, $\tilde{\Lambda}_- = \tilde{\Lambda}(\tilde{q}_x=\tilde{k}_-)$, $\tilde{\Lambda}(\tilde{q}) = \tilde{q}e^{-\tilde{q}^2}/2$, $I_\pm(\nu) = (\int_0^{\tilde{k}_{F\nu}+\tilde{k}_x} d\tilde{k}_- \pm \int_0^{\pm(\tilde{k}_{F\nu}-\tilde{k}_x)} d\tilde{k}_-)$, and $K_\nu = \tilde{k}_{c\nu} cc' + \tilde{k}_{s\nu} ss' + \tilde{k}_{sc\nu}(\tilde{q}^2_x - \tilde{q}_y\tilde{q}'_y)\mathrm{sinc}(\tilde{q}_y+\tilde{q}'_y)$. For $\nu=2$ we have $\varepsilon^{co}_{0,k_x,-1} \approx \varepsilon^{co}_{0,k_x,1}$ and $\varepsilon^{ex}_{0,k_x,-1} \approx \varepsilon^{ex}_{0,k_x,1}$.

Our calculations show that correlations due to bulk screening are weak whereas those due to screening at the edges are strong. For example, as shown in Fig. 4 for sample 1 of Ref. 7 with $\nu=1$, correlations in the middle of the channel change the exchange-corrected energy by about 10% whereas near the channel edges they change it by about 90% as they bring the energy from -0.55 to -0.05. This is due to the fact that, at temperature $T=0$ K, the intra-level screening, the main part of the total screening, comes mainly from transitions near the Fermi edge. Therefore, we obtain a strong correlation near the Fermi edge and a weak one at the channel center. Also, in Fig. 4, the Fermi-edge slope of the exchange-correlation correction is much flatter than that of the exchange. This means that the singularity of the exchange is cancelled by that of the correlation. To show this more clearly we consider the Fermi-edge slopes of the exchange-correlation,

$$\begin{aligned} v^{ec}_g(k_{F\nu}) &= \frac{l}{\hbar}\frac{\partial}{\partial \tilde{k}_x}\varepsilon^{ec}_{0,k_x,\sigma}\big|_{k_x\to k_{F\nu}} \\ &= \frac{l\tilde{\omega}r_0}{2\pi}\Bigg[K_0(\tilde{k}^2_0/4) - \frac{\nu\alpha_0 K_+(\tilde{k}_0)\tilde{K}_{+,\nu}(\tilde{k}_0)}{1+\nu\alpha_0\tilde{K}_{+,\nu}(\tilde{k}_0)} \\ &\quad - \frac{\nu\alpha_0 K_-(\tilde{k}_0)\tilde{K}_{-,\nu}(\tilde{k}_0)}{1+\nu\alpha_0\tilde{K}_{-,\nu}(\tilde{k}_0)}\Bigg]\Bigg|_{\tilde{k}_0\to 0} \\ &\approx v^{HA}_g(k_{F\nu})/\nu. \end{aligned} \tag{13}$$

In deriving Eq. (13) the contribution from the other edge, i.e., the $\int_0^{\tilde{k}_{F\nu}+\tilde{k}_x} d\tilde{k}_- \cdots$ term in Eq. (11), has been neglected. Making use of Eq. (A4), cf. Appendix A, and neglecting the small influence of the sample parameters on the Fermi-edge group velocity[9] led to the final result of Eq. (13) with $v^{HA}_g(k_{F\nu}) = l\Omega^2\tilde{k}_{F\nu}/\tilde{\omega}$. Notice that the first term in the square brackets of Eq. (13) results from the exchange energy, while the other terms result from the correlation energy. For $\nu=2$ the factor $1/\nu$ in (13) is due to the fact that the total screened interaction results from both spin-up and spin-down electrons whereas the exchange-correlation correction results from the exchange of electrons having the same spin. Also, for a given QW sample with fixed width W, we have $k_{F1} = k_{F2}/\sqrt{2}$ and $v^{HA}_g(k_{F2}) = 2v^{HA}_g(k_{F1})$, which gives $v^{ec}_g(\nu=1,\tilde{k}_{F1}) \approx v^{ec}_g(\nu=2,\tilde{k}_{F2})$.

B. $\nu=3$

To see the many-body effects on the $\nu=3$ QHE state, we calculate the exchange-correlation correction to the energy of the occupied $(n=1,\sigma=1)$ LL. In this case Eq. (5) leads to

$$\varepsilon^{\rm ec}_{1,k_x,1}=\varepsilon^{\rm ec1}_{1,k_x,1}+\varepsilon^{\rm ec2}_{1,k_x,1}, \tag{14}$$

where $\varepsilon^{\rm ec1}_{1,k_x,1}$ is the exchange-correlation correction due to charge exchange within the $(n=1,\sigma=1)$ LL and $\varepsilon^{\rm ec2}_{1,k_x,1}$ that due to charge exchange between this LL and the lowest one $(n=0,\sigma=1)$. Using $V^s_3=v_0\delta(q_y+q'_y)/q+V^s_{c3}$ we further decompose each of them into two parts denoted below by the superscripts coi and exi, $i=1,2$. With $Q_{-2}=Q_2(\tilde{q}_x=\tilde{k}_-)$ the results are

$$\varepsilon^{\rm co1}_{1,k_x,1}=-2\overline{v_0}I_-(3)\int\int d\tilde{q}_y\,d\tilde{q}'_y \times e^{i(\tilde{q}_y+\tilde{q}'_y)\tilde{k}_+/2}K_3\tilde{\Lambda}_-\tilde{\Lambda}'_-Q_{-2}Q'_{-2}/\tilde{q}^2_-\tilde{q}'^2_-, \tag{15}$$

$$\varepsilon^{\rm ex1}_{1,k_x,1}=-\overline{v_0}I_+(\nu)\int d\tilde{q}_y\tilde{\Lambda}_-Q^2_{-2}/\tilde{q}^2_-, \tag{16}$$

$$\varepsilon^{\rm co2}_{1,k_x,1}=-\overline{v_0}I_-(3)\int\int d\tilde{q}_y\,d\tilde{q}_y\,e^{i(\tilde{q}_y+\tilde{q}'_y)\tilde{k}_+/2} \times(-\tilde{k}_-+i\tilde{q}_y)(-\tilde{k}_-+i\tilde{q}'_y)K_3\tilde{\Lambda}_-\tilde{\Lambda}'_-/\tilde{q}^2_-\tilde{q}'^2_-, \tag{17}$$

$$\varepsilon^{\rm ex2}_{1,k_x,1}=-(\overline{v_0}/2)I_+(\nu)\int d\tilde{q}_y\,\tilde{\Lambda}_-. \tag{18}$$

The Fermi-edge group velocity can be obtained from Eqs. (14) to (18). Actually Eqs. (16) and (18) show that near the Fermi edge the total exchange correction has a divergent slope $v^{\rm ex}_g(\tilde{k}_{\rm F3})=(\alpha_0/2)v^{\rm HA}_g(\tilde{k}_{\rm F3})K_0(\tilde{k}^2_0/4)|_{\tilde{k}_0\to 0}$. This singularity is exactly cancelled by the Fermi-edge slope of the correlation correction to the $(n=1,\sigma=1)$ LL. To see this, we calculate $v^{\rm co1}_g(k_{\rm F3})$ and $v^{\rm co2}_g(k_{\rm F3})$. The results are $v^{\rm co2}_g(k_{\rm F3})=0$ and

$$v^{\rm co1}_g(k_x\to k_{\rm F3})=\frac{\tilde{l}}{\hbar}\frac{\partial}{\partial\tilde{k}_x}\varepsilon^{\rm co1}_{1,k_x,1}|_{\tilde{k}_x\to\tilde{k}_{\rm F3}}\approx v^{\rm HA}_g(k_{\rm F3})\frac{\alpha_0}{2} \times\left[-K_+-K_-+1+\sum_{i=c,s}\frac{\zeta_i}{\alpha_0\Delta_{i2}+3/2}\frac{K_\pm}{\kappa_\pm}\right], \tag{19}$$

with ζ_i and $\kappa_\pm$ given in Appendix C. With the help of Eq. (A4) we obtain a nonsingular slope at the Fermi edge. For sample 1 of Ref. 7, this nonsingular slope, which is also the overall exchange-correlation slope, is $v^{\rm ec}_g(\tilde{k}_{F3})\approx 3.2v^{\rm HA}_g(\tilde{k}_{\rm F3})$ and agrees very well with the numerical result $v^{\rm ec}_g=3.6v^{\rm HA}_g(\tilde{k}_{\rm F3})$ obtained from Eq. (14). Based on the relationship $v^{\rm HA}_g(\tilde{k}_{F1})=v^{\rm HA}_g(\tilde{k}_{F2})/2=v^{\rm HA}_g(\tilde{k}_{\rm F3})/3\ldots$, we have $v^{\rm ec}_g(k_{F3})>v^{\rm ec}_g(k_{F1})$. This means that the nonsingular part of the correlation correction for $\nu=3$ is larger than that for $\nu=1$. As the screened field $V^s_{c\nu}$ weakens the bare Coulomb field, it follows that a strong nonsingular part of V^s_c entails a weak screened field $|V^s_c|$, that is, $|V^s_{c3}|$ should be smaller than $|V^s_{c1}|$. In other words, the induced charge densities corresponding to these two screened fields should satisfy the relation $\rho_{1,1}<\rho_{0,0}$, where $\rho_{n,n}(n=0,1)$ is the charge density caused by the intra-level transitions within the nth LL. This is true because our previous result $P_{s3}=2+Q_2Q'_2$ in Sec. III shows that transitions within the $n=1$ LL are slightly weaker than those within the $n=0$ LL.[16] That is, the screening "efficiency" in the $n=1$ LL is lower than that in the $n=0$ LL. This is because in the later case $(n=0)$ the electrons are centered at $y=y_0(k_{xi})$ $(i=1,2)$ whereas in the former case $(n=1)$ they are centered at $y=y_0(k_{xi})\pm l$. Therefore, the magnitude of the diagonal matrix element of Eq. (4) for $n=0$ is larger than that for $n=1$. Furthermore, we can predict that for larger n the magnitude of Eq. (4), actually the overlap of the two Fock states centered at different places in phase space, will exhibit an oscillatory behavior when the distance of the two electron centers is increased. The amplitude of the oscillation can be approximated as the overcross of the two displaced Planck-Bohr-Sommerfeld (PBS) bands that represent the two displaced Fock states.[17]

The many-body effects on the $n=1,\sigma=1$ LL of sample 2 of Ref. 7 are not investigated in this work. This is because in this QW sample the bare confining potential V_y around $W/2$ is complicated and invalidates the assumptions used in this work.

V. SINGLE-PARTICLE ENERGY, FERMI-EDGE GROUP VELOCITY

In line with the local-density approximation, as applied to quantum wires,[8] we assume that the single-particle energy can be obtained approximately by solving the Schrodinger equation with Hamiltonian $H=h^0+V_{\rm EC}(y)$, where the exchange-correlation potential is

$$V_{\rm EC}(y)\approx\varepsilon^{\rm ec}_{n,y/l^2,\sigma}=\varepsilon^{\rm ec}_{n,k_x,\sigma},\quad |y|\leqslant W/2. \tag{20}$$

For the region $|y|>W/2$ we take $V_{\rm EC}(y)=0$. In strong magnetic fields $V_{\rm EC}(y)$ is small compared to h^0 and the corresponding eigenvalue can be obtained by

$$E_{n,k_x,\sigma}=\varepsilon_{n,k_x,\sigma}+\langle|V_{\rm EC}(y)|\rangle. \tag{21}$$

In Figs. 5(a)–5(c) we plot the single-particle energies, given by Eq. (21), for the parameters of sample 1 of Ref. 7 and $\nu=1,2,3$, respectively. They agree well with the experimentally observed results of Ref. 7. The parameters for Fig. 5(a) are $\hbar\Omega\approx 0.65$ meV, $W\approx 0.30$ μm, $B=B_1=10$ T, and $\tilde{k}_{\rm F}=\tilde{k}_{\rm F1}=15$.[8] As the correlation correction strongly suppresses the exchange-induced spin-splitting, the quasi-Fermi level of the filled $(n=0,\uparrow)$ LL is above the bottom of the empty $(n=0,\downarrow)$ LL and the $\nu=1$ plateau is absent in sample 1. When the magnetic field is decreased to $B=B_1/2=5$ T in Fig. 5(b), the $(n=0,\uparrow\&\downarrow)$ LLs are fully occupied and there is a big gap $(\sim\hbar\tilde{\omega})$ between the filled $n=0$ LL and the empty $n=1$ LL. Consequently, a $\nu=2$ QHE state exists in this QW sample. For $\nu=3$ we reach the same conclusion as for $\nu=1$. Therefore, electronic correlations suppress the gap between the up and down spin sublevels for $\nu=1$ or $\nu=3$ and *destroy* the quantum Hall plateau;[1] in contrast, they cannot

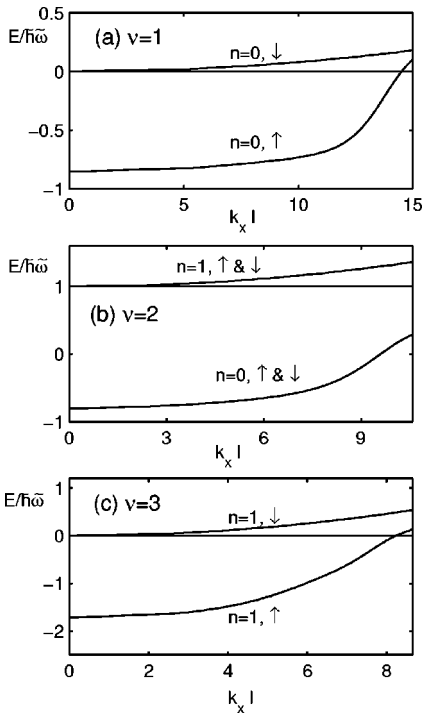

FIG. 5. Single-particle energies, $E_{n,k_x,\sigma}=\varepsilon_{n,k_x,\sigma}+\langle\varepsilon^{\rm ec}_{n,k_x,\sigma}\rangle$ vs $\tilde{k}_x$ for filling factors $\nu=1,2,3$ and the parameters of sample 1 of Ref. 7. The curves for $\nu=1,2$ are shifted downward by 1/2 and those for $\nu=3$ by 3/2.

close the *sizable* gap for $\nu=2$ and this plateau is observed.[7] Figure 6 gives another conclusion for sample 2 with $\nu=1$, $\hbar\Omega=(0.46\pm0.2)$ meV, $W\approx0.33$ μm, $B=B_1\approx7.3$ T, and $\tilde{k}_{\rm F}=\tilde{k}_{\rm F1}=15$. As the correlation is not strong enough to suppress the exchange-induced spin-splitting, there is an activation gap ($\Delta E_{\rm F\downarrow}\approx0.013\hbar\omega_c=1.5$ K) between the occupied $n=0,\uparrow$ and the empty $n=0,\downarrow$ LLs. This is very close to the experimental observation[7] $\Delta E_{\rm F\downarrow}\approx1$ K. Then a $\nu=1$ plateau develops. For $\nu=2$ we have the same conclusion as for sample 1.

The dispersions in Figs. 5 and 6 also give us the single-particle group velocity at the Fermi edge. For example, we have $v_g(k_{\rm F1})\approx6.9\,v_g^{\rm H}(k_{\rm F1})$,[9] $v_g(k_{\rm F2})\approx3.1\,v_g^{\rm H}(k_{\rm F2})$, and $v_g(k_{\rm F3})\approx2.2v_g^{\rm H}(k_{\rm F3})$ for sample 1; for sample 2 the results are $v_g(k_{\rm F1})\approx10\,v_g^{\rm H}(k_{\rm F1})$[9] and $v_g(k_{\rm F2})\approx4.1\,v_g^{\rm H}(k_{\rm F2})$. The relation $v_g(k_{\rm F\nu})-v_g^{\rm H}(k_{\rm F\nu})\propto(d/dy)\langle|V_{\rm EC}(y)|\rangle>0$ confirms that in these two submicron channels the overall exchange-correlation correction has no contribution to the flattening of the outmost edge state, although the exchange-induced spin-splitting is strongly suppressed by the correlations.

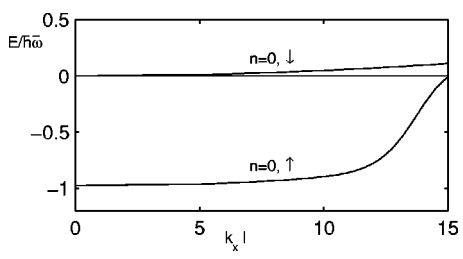

FIG. 6. Same as in Fig. 5 with parameters pertinent to sample 2 of Ref. 7. In contrast with sample 1, when exchange-correlations are taken into account an energy gap appears between the filled $\sigma=1$ sublevel and the empty $\sigma=-1$ sublevel; this leads to the $\nu=1$ QHE state.

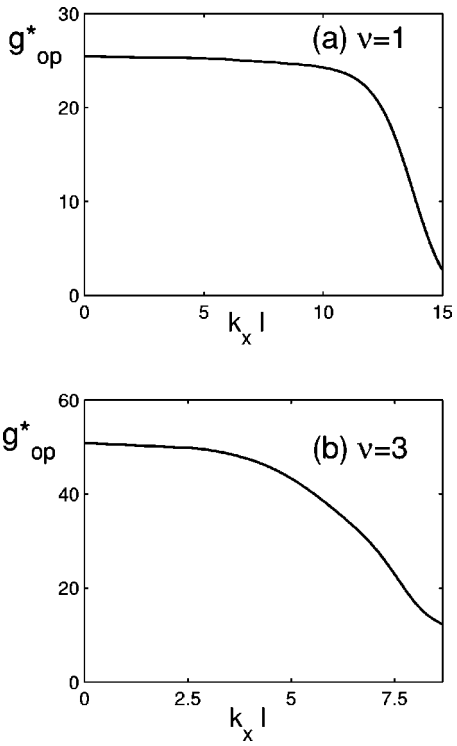

FIG. 7. The effective g factor $g^*_{\rm op}$ vs $\tilde{k}_x$ for sample 1 of Ref. 7 and filling factor $\nu=1$ in (a) and $\nu=3$ in (b). The bare g factor of GaAs is $|g_0|=0.44$.

Finally, we calculate the effective g-factor using the expression

$$g^*_{\rm op}=(E_{n,k_x,-1}-E_{n,k_x,1})/\mu_B B, \tag{22}$$

as a function of $\tilde{k}_x$. We call the g-factor $g^*_{op}(k_x)=g^*_{op}[y_o(k_x)]$ ''optical'' because it is related to the spin splitting between states with the same k_x. It differs from $g_{\rm ac}$[7] deduced from the activated behavior of the conductance. As shown in Fig. 7, for ν odd, $g^*_{\rm op}$ varies strongly across the channel, i.e., from center to edge. For ν even, e.g., $\nu=2$, we have $g^*_{\rm op}=|g_0|$, provided the Zeeman splitting has a negligible effect on the coefficient $F^{\sigma}_{\alpha,\beta}$.

VI. CONCLUDING REMARKS

We investigated the screened Coulomb fields in submicron QWs and their effects on the subband structure within the SHFA-RPA approximation. In strong magnetic fields the integral equation for the screened potential can be simplified by considering only the intra-level and adjacent-level screening. The later contributes a small part to the screened potential, while the former tends to diverge in the long-range limit. One important feature of our approach is that it is free from the usual limitation $r_0\ll1$ of perturbative treatments. With

some extra work it can be applied to situations described by $\nu \geqslant 4$ provided the magnetic field is strong enough and the dimensionless Fermi wavenumber $\tilde{k}_{\mathrm{F}\nu}$ is large enough.

We calculated the exchange-correlation corrections to the energy of the highest occupied LLs. Since the intra-level screening, the main part of the total screening, takes place near the Fermi edge, the correlation energy near the channel edge is much stronger than that at the channel center and strongly suppresses the exchange-induced spin-splitting.

Near the Fermi edge the exchange correction has a positive and logarithmically divergent slope with respect to $\tilde{k}_x$. It is cancelled exactly by the divergent part of the correlation correction to the same LL. The overall Fermi-edge group velocity, $v_g^{\mathrm{ec}}(\tilde{k}_{\mathrm{F}\nu})$, is caused by the nonsingular part of the correlation that is related to the intra-level screened potential. This Fermi-edge group velocity is proportional to the Hartree velocity $v_g^{\mathrm{H}}(\tilde{k}_{\mathrm{F}\nu})$ with the proportionality constant depending on ν. For $\nu=3$ the correlation $\varepsilon^{co}_{1,\tilde{k}_x,1}$ can be further decomposed in two parts: one part corresponds to charge exchange within the same LL ($n=1,\sigma=1$) and the other one to charge exchange between this LL and the adjacent one ($n=0,\sigma=1$). The latter is relatively small and has zero slope at the Fermi edge. The overall Fermi-edge exchange-correlation slope for $\nu=3$ is much larger than that for $\nu=1$, because the induced charge density for $\nu=3$ is relatively smaller than that for $\nu=1$ and this results in the relatively weak field, $|V^s_{c3}|$.

Further, we obtained the single-particle energy in the mean-field-theory spirit of the LDA. Compared to the effective confining potential the impact of the exchange-correlation correction is relative small and the single-particle energies are approximately obtained by Eq. (21). Our calculation accounts well for the experimentally observed[7] strong suppression of the exchange-induced spin-splitting pertinent to integral quantum Hall effect states ($\nu=1$, and $\nu=3$). Near the channel edge the single-particle group velocity has its minimum value, v_g^m, for $k_x \to k_{\mathrm{F}\nu}$. The value v_g^m is larger than $v_g^{\mathrm{H}}(k_{\mathrm{F}\nu})$; this means that in the two narrow QWs of Ref. 7 the exchange-correlation does not contribute to the flattening of the edge state. The results of Eq. (21) also lead to the spatially inhomogeneous effective g-factor, $g_*^{\mathrm{op}}(k_x)$, which varies in the range of 3–25 (10–50) for $\nu=1(3)$, from center to edge.

ACKNOWLEDGMENTS

This work was supported by the Canadian NSERC Grant No. OGP0121756.

APPENDIX A: APPROXIMATE ANALYTIC SOLUTION FOR $\nu=1,2$

Following the approach of Ref. 9 we obtain the values of the various coefficients appearing in Eq. (10) by substituting this trial solution into Eq. (8) and equating the coefficients of each mode on both sides of Eq. (8). The results are as follows:

$$\tilde{k}_{i\nu}(\tilde{q}_x,\tilde{q}_y,\tilde{q}_y')=\frac{-(\pm)\nu\alpha_0}{1+\nu\alpha_0\tilde{K}_{\pm,\nu}}\frac{1}{1+\nu r_0\tilde{\Lambda}}\left[1-\frac{\nu r_0 X\tilde{\Lambda}'}{1+2\nu r_0\tilde{\Lambda}'}\right] \tag{A1}$$

and

$$\tilde{k}_{sc\nu}(\tilde{q}_x,\tilde{q}_y,\tilde{q}_y')=-\frac{X\nu r_0}{\pi(1+2\nu r_0\tilde{\Lambda})}. \tag{A2}$$

Here $\tilde{\Lambda}=\tilde{q}e^{-\tilde{q}^2/2}/2$, $+(-)$ corresponds to $i=c(s)$, $\alpha_0=r_0(\tilde{\omega}/\Omega)^2/(\pi\tilde{k}_{\mathrm{F}\nu})$, and X is a fitting factor for $\nu=1,2$. Comparing the analytical solution, given by Eqs. (10), (A1), and (A2), with the numerical one, we obtain a 80%–90% agreement with $X=1$, depending on the value of q_x. A better agreement can be obtained if we take $X=(2/\pi)\arctan[(\tilde{q})_x^2\cosh(1+2(3\tilde{q}_x)^2)$. An obvious impact of this fitting factor is that we should take $\tilde{k}_{sc\nu}|_{\tilde{q}_x\to 0}\to 0$ for inter-level screening. Notice that in the small $\tilde{q}$ region, the sinc mode only accounts for a small part of the total field. The factor $\tilde{\Lambda}$ in Eq. (A1) means that X has nearly no effect on the intra-level screening in both the short and long wavelength limits. Because X jumps from zero to one within $0.1<\tilde{q}_x<0.5$, the region where X has the stronger influence is $\tilde{q}_x\sim 0.1$. Our numerical computations confirm that the fitting factor can effectively reduce the error of the analytic solution around this region in which its accuracy is worst if we take $X=1$.

The expression for $\tilde{K}_{\pm,\nu}$ in Eq. (A1) is important for understanding the Fermi-edge slope of the exchange-correlation. With $C_\nu(\tilde{q}_y)=1\pm\cos 2\tilde{k}_{F\nu}\tilde{q}_y$ we have[9]

$$\begin{aligned}\tilde{K}_{\pm,\nu}(\tilde{q}_x)&=\int_{-\infty}^{\infty}\frac{d\tilde{q}_y\tilde{\Lambda}C_\nu(\tilde{q}_y)}{\tilde{q}^2(1+\nu r_0\tilde{\Lambda})},\\ &=K_\pm(\tilde{q}_x)-r_0\nu\int_{-\infty}^{\infty}\frac{d\tilde{q}_y\tilde{\Lambda}^2C_\nu(\tilde{q}_y)}{\tilde{q}^2(1+\nu r_0\tilde{\Lambda})},\end{aligned} \tag{A3}$$

$$K_\pm(\tilde{q}_x)\approx[e^{\tilde{q}_{x'}^2/4}K_0(\tilde{q}_x^2/4)/2\pm K_0(2\tilde{k}_{\mathrm{F}}\tilde{q}_x)]e^{-\tilde{q}_x^2/2}, \tag{A4}$$

where $K_0(x)$ is the modified Bessel function. Also, for the confined potential used in this work the dimensionless wavenumber is $\tilde{k}_{\mathrm{F}\nu}=W/2l\sqrt{\nu}$.

APPENDIX B: APPROXIMATE ANALYTIC SOLUTION FOR $\nu=3$

The coefficients $\tilde{k}_{c3}$, $\tilde{k}_{s3}$, and $\tilde{k}_{sc3}$ appearing in Eq. (10) are assumed to have the forms ($Q_j=1-\tilde{q}^2/j, j=2,4; i=c,s;$)

$$\tilde{k}_{i3}=2k_i+k_{iy}Q_2+k_{iy'}Q_2'+k_{iyy'}Q_2Q_2' \tag{B1}$$

$$\tilde{k}_{cs3}=k_{cs}[1+Q_4Q_4'], \tag{B2}$$

where $k_{cs}(\tilde{q}_x,\tilde{q}_y,\tilde{q}_y')$, $k_i(\tilde{q}_x,\tilde{q}_y,\tilde{q}_y')$, $k_{iy}(\tilde{q}_x,\tilde{q}_y,\tilde{q}_y')$, $k_{iy'}(\tilde{q}_x,\tilde{q}_y,\tilde{q}_y')$, and $k_{iyy'}(\tilde{q}_x,\tilde{q}_y,\tilde{q}_y')$ can be determined by using the approach in Appendix A. After a straightforward but tedious derivation we obtain ($i=c:+;i=s:-;$)

$$k_i=-\frac{\pm\alpha_0 D_1(\tilde{q}_x,\tilde{q}_y)D_2(X_3,\tilde{q}_x,\tilde{q}_y')}{1+\alpha_0[2\kappa_\pm+\gamma_i(\kappa_\pm-\Delta_{i1})]}, \tag{B3}$$

$$D_1(\tilde{q}_x,\tilde{q}_y)=[1+2r_0[1+Q_4^2]\tilde{\Lambda}]^{-1}, \tag{B4}$$

$$D_2(X_3,\tilde{q}_x,\tilde{q}_y')=\left[1-\frac{2X_3r_0[1+Q_4']\tilde{\Lambda}'}{1+4r_0[1+Q_4']\tilde{\Lambda}'}\right], \tag{B5}$$

$$k_{iy}=\frac{-2\alpha_0(\kappa_\pm-\Delta_{i1})}{1+\alpha_0(\kappa_\pm-2\Delta_{i1}+\Delta_{i2})}k_i\equiv\gamma_i k_i, \tag{B6}$$

$$k_{iyy'}=\frac{\mp\alpha_0 D_1(\tilde{q}_x,\tilde{q}_y)D_2(X_3,\tilde{q}_x,\tilde{q}_y')}{1+\alpha_0[\lambda_i(\kappa_\pm-\Delta_{i1})+\kappa_\pm-2\Delta_{i1}+\Delta_{i2}]}, \tag{B7}$$

$$k_{iy'}=\frac{-2\alpha_0(\kappa_\pm-\Delta_{i1})}{1+2\alpha_0\kappa_\pm}k_{iyy'}\equiv\lambda_i k_{iyy'}, \tag{B8}$$

where

$$\kappa_\pm(\tilde{q}_x)=\int d\tilde{q}_y(\tilde{\Lambda}/\tilde{q}^2)D_1(\tilde{q}_x,\tilde{q}_y)C_3(\tilde{q}_y), \tag{B9}$$

$$\Delta_{i1}(\tilde{q}_x)=\int d\tilde{q}_y\tilde{\Lambda}D_1(\tilde{q}_x,\tilde{q}_y)C_3(\tilde{q}_y)/2, \tag{B10}$$

$$\Delta_{i2}(\tilde{q}_x)=\int d\tilde{q}_y\tilde{q}^2\tilde{\Lambda}D_1(\tilde{q}_x,\tilde{q}_y)C_3(\tilde{q}_y)/4. \tag{B11}$$

$X_3=1-\exp(-\tilde{q}_x^2)$ is the fitting factor for $\nu=3$.

APPENDIX C: NONSINGULARITY OF THE GROUP VELOCITY $V_G^{ec}(\tilde{k}_{F3})$

To investigate the nonsingularity of the group velocity $v_g^{ec}(\tilde{k}_{F3})$, we calculate the Fermi edge slopes of $\varepsilon^{ex}_{1,k_x,1}$, $\varepsilon^{co2}_{1,k_x,1}$, and $\varepsilon^{co1}_{1,k_x,1}$, with respect to $\tilde{k}_x$, as follows. Equations (16) and (18) give the exchange contribution [$\tilde{\Lambda}_y=\tilde{\Lambda}(0,\tilde{q}_y)$]

$$\begin{aligned}v_g^{ex}|_{k_x\to k_{F3}}&=\frac{l}{\hbar}\frac{\partial}{\partial\tilde{k}_x}(\varepsilon^{ex1}_{1,k_x,1}+\varepsilon^{ex2}_{1,k_x,1})|_{\tilde{k}_x\to\tilde{k}_{F3}}\\&=\frac{r_0l\tilde{\omega}}{2\pi}\left[K_0(\tilde{k}_0^2/4)-2\int_0^\infty d\tilde{q}_y\,\tilde{\Lambda}_y(1-\tilde{q}_y^2/2)\right]_{\tilde{k}_0\to0}\\&=\frac{\alpha_0}{2}v_g^H(\tilde{k}_{F3})K_0(\tilde{k}_0^2/4)|_{\tilde{k}_0\to0},\end{aligned} \tag{C1}$$

which is the same form as $v_g^{ex}(k_x\to k_{F\nu})$ for $\nu=1,2$. The Fermi edge group velocity $v_g^{co2}(k_x\to k_{F3})$ can be readily calculated from Eq. (17); the result is

$$\begin{aligned}v_g^{co2}(k_x\to k_{F3})&=\frac{l}{\hbar}\frac{\partial}{\partial\tilde{k}_x}\varepsilon^{co2}_{1,k_x,1}|_{\tilde{k}_x\to\tilde{k}_{F3}}\\&=\frac{r_0l\tilde{\omega}}{\pi}\int d\tilde{q}_y\,d\tilde{q}_y'\frac{\tilde{\Lambda}_y\tilde{\Lambda}_y'}{\tilde{q}_y\tilde{q}_y'}(\tilde{k}_{s3}\\&\quad-\tilde{k}_{c3})\sin2\tilde{k}_{F3}\tilde{q}_y\sin2\tilde{k}_{F3}\tilde{q}_y'\approx0.\end{aligned} \tag{C2}$$

With the help of Eq. (15) as well as the following relations ($i=c:+$, $i=s:-;$);

$$\gamma_i(\tilde{k}_-\to0)=-\frac{2(\kappa_\pm-\Delta_{i1})}{\kappa_\pm-2\Delta_{i1}+\Delta_{i2}+1/\alpha_0}, \tag{C3}$$

$$\lambda_i(\tilde{k}_-\to0)\approx\frac{2\alpha_0(\Delta_{i1}-\kappa_\pm)}{2\alpha_0\kappa_\pm+1}, \tag{C4}$$

$$k_i(\tilde{k}_-\to0)\approx k_{iyy'}(\tilde{k}_-\to0)/2\approx\mp\frac{\alpha_0}{2\alpha_0\Delta_{i2}+3}, \tag{C5}$$

$$(2+\gamma_i)(\kappa_\pm-2\Delta_{i2}+\Delta_{i1})+2(\Delta_{i1}-\Delta_{i2})=\frac{-\gamma_i}{\alpha_0}, \tag{C6}$$

$$(\lambda_i+1)(\kappa_\pm-\Delta_{i1})=-\lambda_i(1/2\alpha_0+\Delta_{i1}), \tag{C7}$$

we have, to order κ_i^0,

$$\begin{aligned}v_g^{co1}(k_x\to k_{F3})&=\frac{l}{\hbar}\frac{\partial}{\partial\tilde{k}_x}\varepsilon^{co1}_{1,k_x,1}|_{\tilde{k}_x\to\tilde{k}_{F3}}\\&\approx\frac{-2r_0l\tilde{\omega}}{\pi}\frac{\partial}{\partial\tilde{k}_x}\bigg|_{\tilde{k}_-\to0}I_-(3)\int_{-\infty}^{\infty}d\tilde{q}_y\,d\tilde{q}_y'\frac{\tilde{\Lambda}_y}{\tilde{q}_y^2}\frac{\tilde{\Lambda}_y'}{\tilde{q}_y'^2}e^{i(\tilde{q}_y+\tilde{q}_y')\tilde{k}_+/2}Q_{-2}Q'_{-2}[\tilde{k}_{c3}cc'+\tilde{k}_{s3}ss']\\&=\frac{r_0l\tilde{\omega}}{2\pi}\sum_{i=c,s}(\pm)[k_i(0)\overline{\eta}_{1i}(K_\pm+\Gamma_{\pm1})+2k_{iyy'}(0)\overline{\eta}_{3i}(K_\pm+2\Gamma_{\pm1}+\Gamma_{\pm2})]\\&\approx v_g^H(k_{F3})\frac{\alpha_0}{2}\left[-K_+-K_-+1+\sum_{i=c,s}\frac{\zeta_i}{\alpha_0\Delta_{i2}+3/2}\frac{K_\pm}{\kappa_\pm}\right]_{\tilde{k}_-\to0}.\end{aligned} \tag{C8}$$

Here

$$\Gamma_{\pm 1} \equiv -\int_0^\infty d\tilde{q}_y \tilde{\Lambda}_y (1 \pm \cos 2\tilde{k}_F \tilde{q}_y) \approx -0.5,$$

$$\Gamma_{\pm 2} \equiv \frac{1}{2}\int_0^\infty d\tilde{q}_y \tilde{q}_y^2 \tilde{\Lambda}_y (1 \pm \cos 2\tilde{k}_F \tilde{\lambda}_y) \approx 0.5, \qquad \text{(C9)}$$

$\bar{\eta}_{1i} = (2+\gamma_i)\kappa_\pm - 2\Delta_{i1}(1+\gamma_i) + \gamma_i \Delta_{i2}$, $\bar{\eta}_{3i} = (\lambda_i + 1)\kappa_\pm - \Delta_{i1}(\lambda_i + 2) + \Delta_{i2}$, and $\zeta_i = \Delta_{i2} - \Delta_{i1} + 1/\alpha_0 + \alpha_0(\Delta_{i1} + 1/2\alpha_0)^2$. Therefore the total group velocity, including $v_g^{\rm ex}(k_{\rm F3})$, is

$$v_g^{\rm ec}(k_{\rm F3}) \approx v_g^{\rm H}(k_{\rm F3}) \frac{\alpha_0}{2}\left[1 + \sum_{i=c,s} \frac{\zeta_i}{\alpha_0 \Delta_{i2} + 3/2} \frac{K_\pm}{\kappa_\pm}\right]. \qquad \text{(C10)}$$

†Electronic address: zxzhang@boltzmann.concordia.ca
*Electronic address: takis@boltzmann.concordia.ca

[1] D.B. Chklovskii, B.I. Shklovskii, and L.I. Glazman, Phys. Rev. B **46**, 4026 (1992).
[2] B.Y. Gelfand and B.I. Halperin, Phys. Rev. B **49**, 1862 (1994); G. Muller, D. Weiss, A.V. Khaetskii, K. von Klitzing, S. Koch, H. Nickel, W. Schlapp, and R. Losch, *ibid.* **45**, 3932 (1992).
[3] J. Dempsey, B.Y. Gelfand, and B.I. Halperin, Phys. Rev. Lett. **70**, 3639 (1993); Surf. Sci. **305**, 166 (1994).
[4] L. Brey, J.J. Palacios, and C. Tejedor, Phys. Rev. B **47**, 13 884 (1993).
[5] J.M. Kinaret and P.A. Lee, Phys. Rev. B **42**, 11 768 (1990).
[6] T. Suzuki and T. Ando, J. Phys. Soc. Jpn. **62**, 2986 (1993).
[7] J. Wrobel, F. Kuchar, K. Ismail, K.Y. Lee, H. Nickel, W. Schlapp, G. Grobecki, and T. Dietl, Surf. Sci. **305**, 615 (1994).
[8] O.G. Balev and P. Vasilopoulos, Phys. Rev. B **56**, 6748 (1997).
[9] Z. Zhang and P. Vasilopoulos, J. Phys.: Condens. Matter **13**, 1539 (2001).
[10] O.G. Balev and N. Studart, Phys. Rev. B **64**, 115309 (2001).
[11] O.G. Balev and P. Vasilopoulos, Phys. Rev. B **56**, 13 252 (1997); **59**, 2807 (1999).
[12] T. Ando and Y. Uemura, J. Phys. Soc. Jpn. **37**, 1044 (1974).
[13] C. Kallin and B.I. Halperin, Phys. Rev. B **30**, 5655 (1984); M.M. Fogler and B.I. Shklovskii, *ibid.* **52**, 17 366 (1995); R.J. Nicholas, R.J. Haug, K. Von Klitzing, and G. Weimann, *ibid.* **37**, 1294 (1988); W. Xu, P. Vasilopoulos, M.P. Das, and F.M. Peeters, J. Phys.: Condens. Matter **7**, 4419 (1995).
[14] S. Chaturvedi, G.J. Milburn, and Z. Zhang, Phys. Rev. A **57**, 1529 (1998); G.S. Agarwal and K. Tara, *ibid.* **43**, 492 (1991).
[15] This additional phase factor would shift up the exchange-correlation energy by a small amount. For example, for the parameters of sample 1 in Ref. 7 this energy shift for $\nu = 1$ is less than $\leqslant 0.02\hbar\tilde{\omega}$ at the channel edge and nearly zero in the middle of the channel.
[16] We only consider the intra-level screening parts, since, as shown in Appendix C, the inter-level screening has no contribution to the Fermi-edge slope of the exchange-correlation energy.
[17] W.P. Schleich and J.A. Wheeler, Nature (London) **326**, 574 (1987); J.P. Dowling, W.P. Schleich, and J.A. Wheeler, Ann. Phys. (Leipzig) **7**, 403 (1991).